Developments in Operational Long-Range Climate Prediction at CPC

EDWARD A. O'LENIC, DAVID A. UNGER, MICHAEL S. HALPERT, AND KENNETH S. PELMAN

National Oceanic and Atmospheric Administration/National Weather Service/Climate Prediction Center, Camp Springs, Maryland

(Manuscript received 8 May 2007, in final form 13 September 2007)

ABSTRACT

The science, production methods, and format of long-range forecasts (LRFs) at the Climate Prediction Center (CPC), a part of the National Weather Service's (NWS's) National Centers for Environmental Prediction (NCEP), have evolved greatly since the inception of 1-month mean forecasts in 1946 and 3-month mean forecasts in 1982. Early forecasts used a subjective blending of persistence and linear regression-based forecast tools, and a categorical map format. The current forecast system uses an increasingly objective technique to combine a variety of statistical and dynamical models, which incorporate the impacts of El Niño–Southern Oscillation (ENSO) and other sources of interannual variability, and trend. CPC's operational LRFs are produced each midmonth with a "lead" (i.e., amount of time between the release of a forecast and the start of the valid period) of ½ month for the 1-month outlook, and with leads ranging from ½ month through 12½ months for the 3-month outlook. The 1-month outlook is also updated at the end of each month with a lead of zero. Graphical renderings of the forecasts made available to users range from a simple display of the probability of the most likely tercile to a detailed portrayal of the entire probability distribution.

Efforts are under way at CPC to objectively weight, bias correct, and combine the information from many different LRF prediction tools into a single tool, called the consolidation (CON). CON ½-month lead 3-month temperature (precipitation) hindcasts over 1995–2005 were 18% (195%) better, as measured by the Heidke skill score for nonequal chances forecasts, than real-time official (OFF) forecasts during that period. CON was implemented into LRF operations in 2006, and promises to transfer these improvements to the official LRF.

Improvements in the science and production methods of LRFs are increasingly being driven by users, who are finding an increasing number of applications, and demanding improved access to forecast information. From the forecast-producer side, hope for improvement in this area lies in greater dialogue with users, and development of products emphasizing user access, input, and feedback, including direct access to 5 km × 5 km gridded outlook data through NWS's new National Digital Forecast Database (NDFD).

1. Introduction

This paper describes the rationale, latest methods, and skill of the National Oceanic and Atmospheric Administration's (NOAA) operational 1- and 3-month outlooks, produced at the Climate Prediction Center (CPC) in Camp Springs, Maryland. Operational outlooks of 1-month-mean U.S. temperature, and total precipitation, were first issued, in a categorical format, at zero lead, in 1946 by the U.S. Weather Bureau. Categorical 3-month-mean outlooks for four adjacent seasons began in 1973. Probabilistic, zero-lead outlooks for 3-month-average temperature and total precipitation began in July 1982. Probabilistic 1-month outlooks, at a lead of ½ month, and 3-month outlooks, at leads of ½ month to 12½ months in increments of 1 month, were first issued in mid-December 1994 (Van den Dool 1994; O'Lenic 1994; Barnston et al. 1994). For many years the community has referred to these products as long-range forecasts (LRFs), and this terminology will be used throughout this paper. Also, the term "outlook" is used in reference to the final 1- or 3-month outlook, while "forecast" is used when describing tools used to produce an outlook, or forecasting in general.

While the instantaneous details of the weather are unpredictable beyond a limit of about 2 weeks, statistics such as weekly and longer means, and standard devia-

Corresponding author address: Edward A. O'Lenic, National Centers for Environmental Prediction, W/NP5, Rm. 604 WWB, 5200 Auth Rd., Camp Springs, MD 20746.
E-mail: ed.olenic@noaa.gov

DOI: 10.1175/2007WAF2007042.1

TABLE 1. Evolution of operational LRFs.

Years	Variables (predictands)	Tools	Formulation, lead
1946–81	Surface temperature (*T*); precipitation (*P*); categorical: above (A), below (B), and normal (N)	Linear regression (with 700-hPa height as predictor), persistence of anomalies	Subjective, zero lead
1982–94	*T*, *P*, tropical Pacific SST, A, B, N, and probabilities (%)	Linear regression (with 700-hPa height as predictor), trend, analog–antianalog, ENSO	Mostly subjective, zero lead
1995–2004	*T, P*, SST, A, B, N, %, terciles, and POE	SMLR (with SST, 500-hPa height, surface *T*, *P*, most recent soil moisture, and trend as predictors), OCN, CCA (with SST, 700-hPa height, *T*, and *P* as predictors), ENSO, two-tier coupled model, skill mask (1995), SST, CON	Equal parts subjective/objective, ½–12½-month lead
2004–06	*T, P*, SST, A, B, N, %, terciles, and POE	SMLR, trend, CCA, ENSO, one-tier coupled model (CFS, in 2004), skill mask, *T*, *P*, CON	Mostly objective, ½–12½-month lead

tions, are predictable to some degree (Lorenz 1982). Evaluations of the skill of operational LRFs by Namias (1953) and subsequently Barnston (1994a,b), Barnston et al. (1994, 1999), and Livezey et al. (1995) support this assertion. Blackmon (1976) and Blackmon et al. (1977) have shown that the low-frequency variability of Northern Hemisphere upper-air height shows a tendency for the standard deviation to have minima over land areas and maxima over the oceans downstream of the storm tracks, while the low-frequency variability of near-surface temperature is largest over the continents and at high latitudes. Low-frequency variability of upper-air height was subsequently shown to be associated with stationary teleconnection patterns, which are maintained by energy from the basic state derived from barotropic instability (Simmons et al. 1983; Blackmon et al. 1984a,b). Ocean–atmosphere (Rasmusson and Carpenter 1982) and land–atmosphere interactions (Huang and Van den Dool 1996; Van den Dool 2007; Van den Dool et al. 2003) were also found to produce predictable anomaly patterns. Phenomena that fall into this category include ENSO, trends, and long-lived teleconnection patterns (Wallace and Gutzler 1981; Barnston and Livezey 1987, Horel and Wallace 1981; Livezey and Smith 1999, Mo and Livezey 1986; Higgins et al. 2000a,b; Higgins et al. 2002; Van den Dool 2007). CPC's forecast tools and methods have been developed based upon state-of-the-art knowledge of these phenomena and interactions.

Section 2 describes the forecast tools used in operational seasonal-to-interannual (SI) forecasting at CPC. Section 3 discusses the forecast format and interpretation. Section 4 discusses operational procedures. Section 5 describes the skill of operational LRFs. Section 6 gives conclusions.

2. Overview of forecast methods and tools

Table 1 illustrates the evolution of CPC's LRF operations. Strictly subjective modification and consolidation of forecast tools were practiced during 1946–81. The forecast tools used during that era were based upon the persistence of current anomalies into the forecast period, linear regression, and the skill advantage that can be gained by applying a forecast for the first week from a zero-lead forecast as the forecast for the entire forecast period (Namias 1953; Gilman 1985). This situation began to change during the 1980s, when an appreciation of the dominant influence of El Niño–Southern Oscillation (ENSO) began to emerge (Rasmusson and Carpenter 1982).

ENSO composites, which are averages of observed temperature and precipitation maps stratified by ENSO phase, and expressed as anomalies (Higgins et al. 2000a), were implemented in the 1990s. An understanding was also developed over that decade that trends and other long-time-scale signals have a significant impact on 3-month means. This motivated the development of new statistical forecast tools, such as canonical correlation analysis (CCA; Barnston 1994b) and optimal climate normals (OCN; Huang et al. 1996; Van den Dool 2007), which were found to be skillful at leads out to as long as a year. This long-lead skill from statistical tools and ENSO afforded an increase in the lead time of the forecasts, which was incorporated into CPC's 3-month outlook operations with the outlook prepared in mid-December 1994. Until January 1995, the lead (the amount of time between the release of a forecast and the start of its valid period) was zero. Beginning with the 3-month outlook valid January–March 1995, the lead time of 3-month outlooks was increased to a mini-

mum of 2 weeks and a maximum of 12½ months. Instead of just one temperature and one precipitation map, each outlook would now consist of a set of 13 outlooks, with 26 maps, for leads of ½ to 12½ months, with each lead overlapping the next by 2 months.

The addition of skill masks (Barnston 1994a; Van den Dool 2007) and an objective consolidation of SST forecasts in the mid-1990s (Unger et al. 2008, manuscript submitted to *Mon. Wea. Rev.*, hereafter UVOC) further reduced the amount of subjective input required to prepare the 1- and 3-month outlooks. A method to objectively combine, or "consolidate," four forecast tools for surface temperature and precipitation was implemented in late 2006. This technique resulted in a substantial increase in the skill of hindcasts, in comparison with official outlooks made operationally over the same 10-yr period (1995–2005).

We now briefly describe the forecast tools.

The *climate forecast system* (CFS, implemented 2004; see Table 1*)* is a "one tier", fully coupled, dynamical model of the global oceans and atmosphere. An ensemble of 10 forecasts is run twice each day out to 9 months. The output data from the model are freely and publicly available online via ftp (Saha et al. 2006). In one-tier models, the future evolution of ocean–land–atmosphere interactions is predicted by integrating a fully coupled atmosphere–ocean–land model from realistic initial conditions. There are no flux adjustments between the ocean and atmosphere components of the CFS (Saha et al. 2006). Some dynamical modeling systems use an older, "two tier" scheme in which a coupled ocean–atmosphere model is run in order to acquire a forecast of SSTs (first tier). A second integration is then run, using the SST forecast as the lower ocean boundary for an atmospheric GCM (Ji et al. 1994) (second tier). The primary assumption of two-tier models is that the atmosphere–ocean interaction serves as the major source of skill in the LRFs, and that the evolution of low-frequency ocean–atmosphere interactions is dominated by the ocean, as represented by the SST.

The *optimal climate normals* (OCN, implemented 1995; Table 1) approach uses the arithmetic difference between the 10- (15-) yr mean of the most recently observed seasonal mean temperature (seasonal total precipitation) for a given season and the 30-yr climatology (currently 1971–2000) for that season (the trend) as the forecast for the next realization of that season. The current World Meteorological Organization (WMO) convention is for the climatology to be computed over three adjacent calendar decades, and to update the climatology every 10 yr, near the beginning of a decade. In a changing climate, this means that the trends indicated by tools such as the OCN grow larger as the climatology ages (Van den Dool 1994; Huang et al. 1996).

The *canonical correlation analysis* (CCA, implemented 1994; Table 1) uses linear statistical techniques to find optimum relationships among multivariate sets of independent and dependent variables. CPC's CCA uses 700-hPa height, nearly global SST, and time-lagged U.S. surface temperature or precipitation as predictors at multiple locations, and U.S. surface temperature or precipitation at multiple locations as predictands (Barnston 1994b).

Screening multiple linear regression (SMLR, implemented 1997; Table 1) is used to extract information from two or more variables to produce a forecast of the seasonal and monthly mean temperature and total precipitation. CPC's SMLR predictor variables include Northern Hemisphere 700-hPa height, nearly global SST, U.S. surface temperature (T) or precipitation (P), and soil moisture estimates. SMLR is applied to 102 conterminous U.S. climate divisions (Guttman and Quayle 1996), rather than multistation anomaly patterns, as is done in CCA (Unger 1997).

The *consolidation* (CON, implemented 2006; Table 1) is used to create a single forecast tool that exploits the tendency for the information available in the four main forecast tools (CFS, CCA, OCN, and SMLR) to be, in part, complementary. This quality gives it higher average skill than any of the individual forecast tools (UVOC). It does this by estimating the bias and skill of each tool from available hindcast data and forming a single probabilistic forecast from a weighted combination of the debiased tool forecasts. The weights are proportional to the skill of the tool and represent the independent information contributed by each tool. The hindcasts must come from the operational version of the given tool and, hence, need to be regenerated each time the formulation of a tool is changed. The technique uses an adaptive regression technique, similar to a simplified Kalman filter (Kalman 1960). Also, the consolidation bases its relationships much more heavily on the most-recent 10–15 yr, and is quicker to adapt to trends and other changes in the climate system than, say, CCA and SMLR, whose training datasets cover longer periods (UVOC). A documented tendency for the consolidation to overemphasize the trend is accounted for in CPC operations by detrending the CFS, CCA, and SMLR forecasts prior to consolidation, and then adding in a damped version of the OCN forecast afterward (Huang and Van den Dool 1996).

The CON tool has several advantages. These include 1) replacing the subjective process formerly used to combine forecast tool information with an objective, reproducible method; 2) providing a seasonal forecast

"first guess" with higher average skill than either the individual guidance tools used to create the CON or the official forecasts subjectively formulated from the tools; and 3) providing a methodology that can be used to incorporate additional forecast tools in the future. The considerable enhancement in the skill of forecasts that use consolidation will be discussed in section 5.

The "skill mask" was introduced into CPC's LRF operations in 1995 (Table 1) (Barnston 1994a; Van den Dool 1994). The idea is to display forecast information for a given tool to the forecaster working on the operational outlook only if it has skill, as determined by cross validation, or reforecasting, over at least 25 yr, exceeding some "useful" skill threshold. The skill mask was intended to limit the amount of pure speculation and possible misuse of nonskillful information that could be subjectively incorporated into the official forecast. The skill measure used for the skill masks for the four primary forecast tools (SMLR, CCA, OCN, and CFS) is the anomaly correlation, (AC; Wilks 1995; see the appendix). The minimal skill threshold is chosen as AC = 0.3. (Forecast information displayed at locations on the maps of the forecast tools seen by the forecasters where the AC did not exceed 0.3 over an average of many hindcasts is limited to only the sign of the anomaly.) Colors indicate the category, red for above, blue for below, and green for the middle tercile. (Figs. 7a-d, 8a-d show detailed examples of skill-masked forecast maps.)

3. Forecast format and interpretation

The probabilistic format of CPC's 1- and 3-month outlook maps is necessary to represent the chaotic nature of the climate system, whose monthly and seasonal behavior and patterns are intrinsically not deterministic. CPC's public LRF maps (Fig. 1) use three tercile categories, which are labeled below (B), normal (N) or median, and above (A), and whose chance likelihood is 33⅓% each, estimated using 30 yr of observed data (currently for 1971–2000). For any given location and season, a normal distribution is fitted to the corresponding 30 temperature observations in the climatology period. Precipitation data are transformed to be symmetric about the median, making the transformed distribution approximately normally distributed. The values that divide these distributions into thirds are the two values of the variables corresponding to their (+) and (−) 0.43 standard deviations. The categories on the map correspond to the three subdivisions of the observed distributions of temperature and precipitation that result from this statistical treatment. Under ideal conditions for temperature for example, at any given location, and for any chosen time of year, the coldest 10 yr define the lower third (the below category), the middle 10 yr define the middle third (normal for T and median for P), and the warmest 10 yr define the upper third of the observed distribution (the above category).

CPC operational 1- and 3-month outlooks are simultaneously available in three formats, which provide three levels of information. The first format is the traditional three-class probability map (Fig. 1). The second format shows the amount by which the middle of the distribution shifts as a result of the outlook (Fig. 2). The third format gives the details of the observed and outlook distributions for any of up to 102 climate divisions over the conterminous United States, and is called the probability of exceedance (POE) graph (Fig. 3).

The first format allows three categories, which span all possible values of temperature or precipitation, to be displayed on a single map, as in Fig. 1. To facilitate understanding and for simplicity, we have devised rules that apply to the contours on CPC probabilistic 1- and 3-month outlook maps. At any point on the outlook map (Fig. 1) the likelihood of the three categories sums to 100%. There are 19 sets of unique possible tercile probability combinations for the map contour patterns shown in Table 2. These include a set for even odds (⅓, ⅓, ⅓), six sets for each extreme category (12 in all), and six sets for when the middle category is the most likely. In each case, with the exception of EC, the category and probability plotted on the map (Fig. 1) are those associated with the highest numerical values of the probabilities for the three categories specified by the forecast. This means, in Fig. 1a for example, that along the 50 contour in the Midwest the likelihood of above normal is 50%, while the likelihood of below drops to 16⅔%, and the odds of the middle category remain at 33⅓%. When the odds of above or below reach 63⅓% or higher, the odds of the opposite category reach a minimum allowed value of 3⅓%, while the odds of the middle category are allowed to drop below 33⅓%. In the case where the middle category is favored, the odds of the extreme categories each decline by amounts equal to ½ of the amount by which the middle category exceeds 33⅓. The possible sets of tercile map contour probabilities for this situation are (30, 40, 30), (25, 50, 25), (20, 60, 20), (15, 70, 15), (10, 80, 10), and (5, 90, 5) (Table 2). The last four of these sets are rarely, if ever, used. The EC category is used in 1- and 3-month outlooks, and refers to the case where the odds of all three categories (B, N, and A) are equal, at 33⅓% each.

The probabilities plotted on the maps (Fig. 1) indicate the likelihood of the most likely category among the three. However, the deviation in the likelihood of the three categories from climatology can be translated

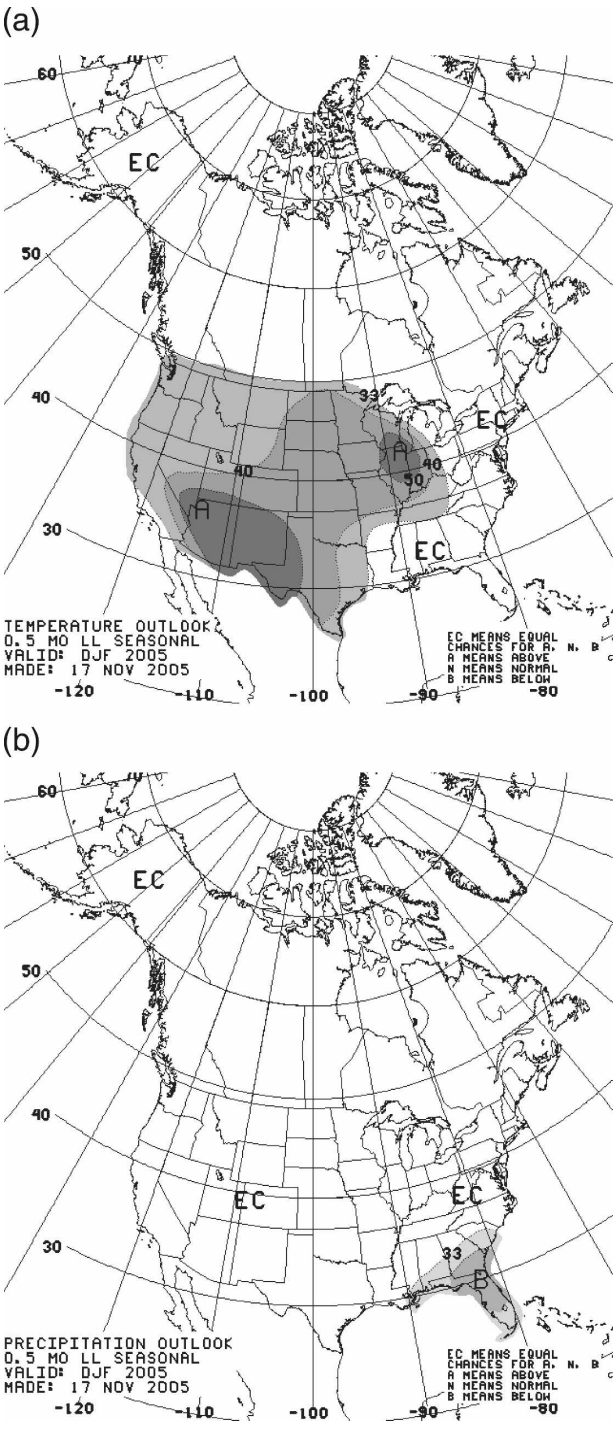


FIG. 1. Long-range (3 month) outlooks of the probability of terciles of (a) *T* and (b) *P* valid DJF 2005–06, made with a lead time of about ½ month. Shaded, contoured areas are the total probability of the indicated category: B stands for below normal, N for normal or median, and A for above normal. EC denotes equal chances (33⅓%) for each of the three possible categories.

into changes in the mean and standard deviation of the original distribution. Because both observed 3-month seasonal mean temperatures and their outlooks are approximately normally distributed, the mean is the most likely single value (this is also done for precipitation, using a transformed version of the distribution, which is symmetric about the median). Thus, the second format is a map (Fig. 2) showing the shift, in degrees for temperature, and in inches for precipitation, in this midvalue of the distribution. This shift is precisely related to the probabilities associated with the forecast (Fig. 1) through probability theory. The shaded solid contours of this parameter indicate the amount of this shift, given as an anomaly from the 1971–2000 climatology, which is shown in dashed contours (Fig. 2).

Expressing the distribution of temperature or precipitation for a given location or climate division as an integral of the probability density starting at the rightmost side of the distribution, and plotting the result in terms of value of the variable versus cumulative probability, gives the probability that the value on the abscissa will be exceeded or, simply, the "probability of exceedance" (POE) curve, also called a survival curve. One such graph, for a climate division in northern Minnesota, is shown for the December–February (DJF) 2005 temperature outlook in Fig. 3. The values of the probability on the outlook maps (Fig. 1) can be read directly from the graph for the variable of interest for each of 102 climate divisions over the conterminous United States. Together, these three renderings (Figs. 1–3) give a wide range of interpretations, and quality of information, for the forecast, suitable for a wide range of user applications.

Users of CPC outlook products span a wide range of backgrounds, expertise, and requirements. They have expressed a desire for improved or augmented LRF products that are, among other things, 1) in the form of raw, gridded forecast data; 2) more understandable; 3) more highly resolved in time and space; and 4) available for additional variables (National Research Council 2001, 2003). Resolving these user requirements will necessarily require a dialogue between the producers and users of the products, and the applications community that works to adapt raw forecast products to the needs of a growing user community.

4. Operational LRF procedures

On the third Thursday of each calendar month, at 0830 eastern time, CPC releases its latest 1- and 3-month outlooks. The outlook process begins 6 days earlier, when CPC hosts a Friday telephone–Internet-based conference to discuss the latest forecast tools

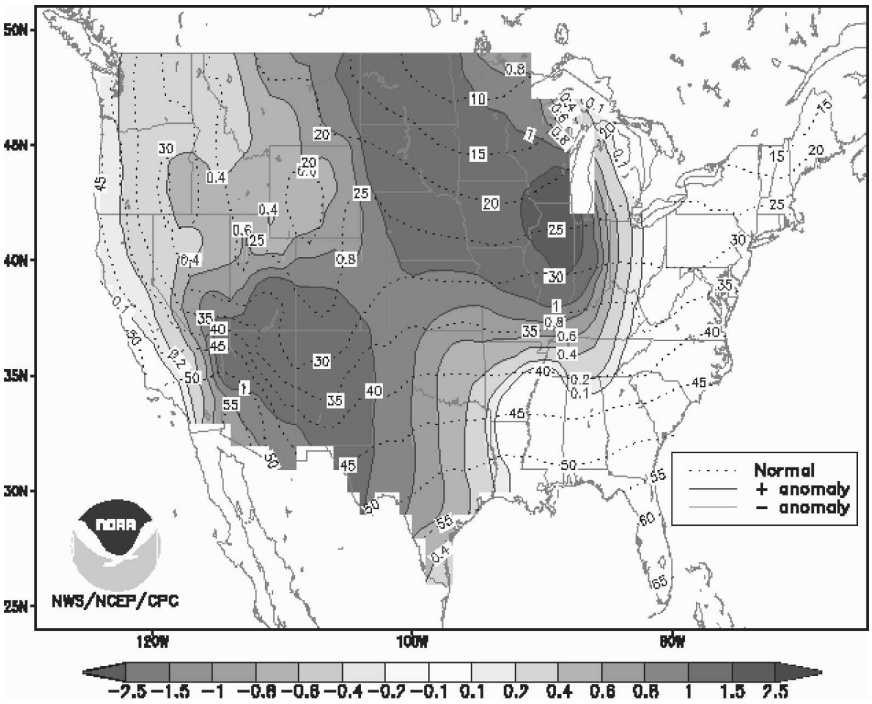


FIG. 2. Anomaly of the midvalue of the 3-month *T* outlook distribution (solid, shaded contours, and labels) for DJF 2005/06. Dashed contours are the climatological 3-month mean *T* (°F).

with partners, including NWS field and regional headquarters personnel. The preparation methods, format, and verification of the 1- and 3-month outlooks are nearly identical. Using the input from this discussion, and the set of forecast tools listed in Table 1, the forecaster drafts a set of outlook three-class probability maps. The maps showing the shift in the center of the distribution and the POE graphs discussed in the previous section are created from the three-class maps via automated processes.

a. The 1-month outlook

CPC's 1-month outlook, valid for a given future calendar month, is prepared twice each month. The first issuance is made at about a 2-week lead, on the third Thursday of the month at the same time as the 3-month outlook. The second issuance is made on the last day of the month at a lead of zero. This two-phase set of outlooks for the same target month is intended to meet the requirements of users who have expressed a desire for either 2-week-lead or zero-lead outlooks. The format of the maps and graphics for this outlook is identical to that of the 3-month outlook (see section 3). The outlook is prepared by a single forecaster using tools appropriate to the lead time (Table 3).

We may contrast the 1-month outlooks made at a 2-week lead, which depend solely on relatively weak climate signals, with those made at zero lead, whose monthly skill can often be boosted significantly by relatively high-skill forecasts of weather events early in the target month, especially precipitation. A sample complete set of these outlooks for the forecasts valid for December 2005 is shown in Fig. 4. The differences in the temperature outlooks between the ½-month and zero-lead versions owe, in part, to the availability to the forecaster of an operational week-2 forecast and other short-range forecasts valid for the early part of the target month.

Zero-lead 1-month outlooks were implemented in August 2004. Their (non-EC) average Heidke skill (percent improvement over climatology) over that period is 35.9 for temperature and 15.7 for precipitation, compared with 30.6 and 7.7 for the ½-month-lead 1-month outlook. The remainder of the paper will focus on the 3-month outlooks.

b. The 3-month outlook

The 3-month outlook preparation process begins with comprehensive analyses of the state of the global oceans and atmosphere (Fig. 5). These analyses are used to initialize or drive a series of dynamical and statistical models of the oceans and atmosphere. The

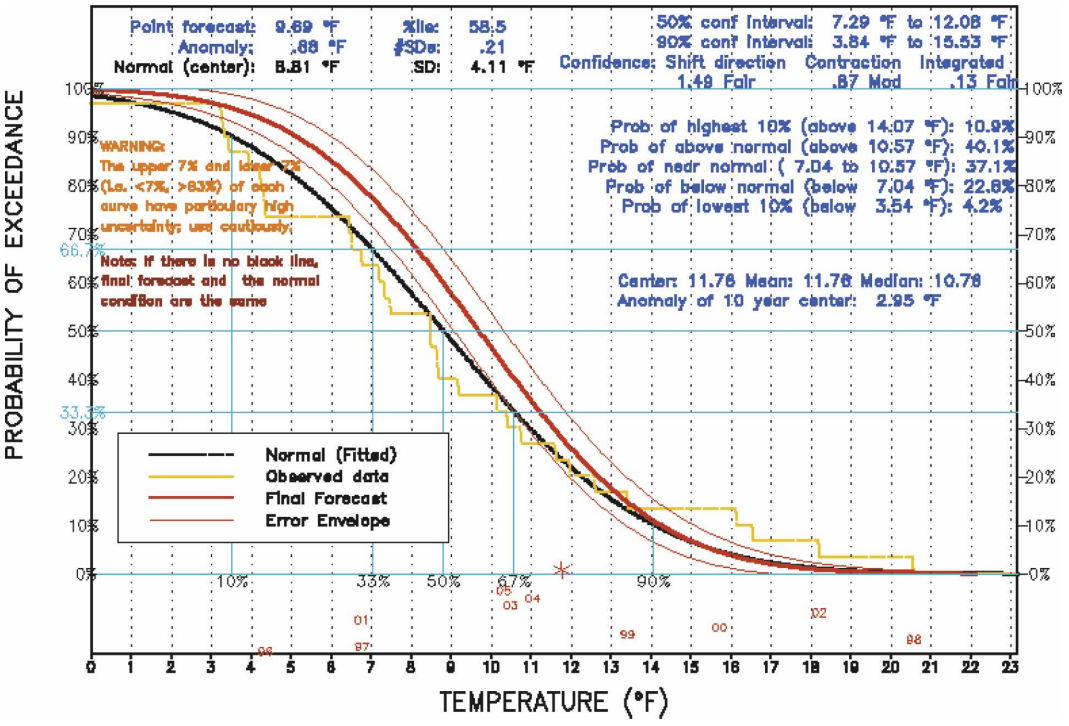


FIG. 3. Survival curves for 1971–2000 observed (yellow curve), a normal distribution fit to the observed (black), and the 3-month temperature outlook distributions (heavy red curve) of T for a climate division near northern MN for DJF 2005–2006. The graphs give the probability (y axis) that the values on the x axis will be exceeded. Horizontal lines indicate the relationship between paired values of temperature and the climatological probability (heavy black curve). The heavy red curve shows the change in the climatology indicated by the outlook for this region. The light red lines straddling the outlook give the likely error associated with the forecast. Annotations in the upper half of the diagram refer to statistical properties of the observed and forecast distributions. Red numbers near the bottom show the observed seasonal mean T for the last 10 yr, while the asterisk shows the mean of these 10 T values.

analyses and forecast tools are placed on a public Web page (http://www.cpc.ncep.noaa.gov/products/predictions/90day/tools/briefing). The forecaster who is to prepare the outlook conducts a telephone conference call, as described earlier, to discuss with our partners in the climate community the current status of the climate system and the content of the available forecast tools. Based on the results of these discussions, and his or her own interpretation of the forecast tools, the forecaster drafts the three-class outlook maps for each of the variables and leads.

The forecaster hosts another telephone conference call on the Tuesday following the first briefing to discuss the draft forecasts with a group of partners within the government. Since the forecast is embargoed from public release until the upcoming Thursday, the participants in this second conference call must agree to maintain the confidentiality of the information (all participants in this process are prohibited, by law, from using this information for their own, or others', financial gain).

The forecaster finalizes the draft outlook maps, based upon input received during the second briefing, and composes a bulletin giving a brief synopsis of the status of the climate system, the rationale behind the forecaster's choices, and an overview of the outlook maps. The 3-month outlook production process culminates with the dissemination of a set of 26 three-month forecast maps (13 each for temperature and precipitation) along with a text bulletin on Thursday (the third Thursday of the month). We will now discuss the 3-month outlook process in the context of the actual forecast for DJF 2005–06, which was disseminated on 17 November 2005.

Among the first steps in the seasonal forecast process is to assess the current and expected future status of the sea surface temperatures in the tropical Pacific. Figure 6 shows the official SST forecast issued 11 November 2005, along with forecasts from the tools used to produce an objective consolidation, indicated by the box-and-whiskers plots. This is the forecast available operationally for preparing the 3-month outlook for DJF

TABLE 2. Possible below, normal, and above combinations on 1- and 3-month outlook probability maps.

No.	Probability of B (%)	Probability of N (%)	Probability of A (%)
1	90	6.67	3.33
2	80	16.67	3.33
3	70	26.67	3.33
4	60	33.33	6.67
5	50	33.33	16.67
6	40	33.33	26.67
7	33.33	33.33	33.33
8	30	40	30
9	25	50	25
10	20	60	20
11	15	70	15
12	10	80	10
13	5	90	5
14	10	80	10
15	15	70	15
16	20	60	20
17	25	50	25
18	30	40	30
19	33.33	33.33	33.33
20	26.67	33.33	40
21	16.67	33.33	50
22	6.67	33.33	60
23	3.33	26.67	70
24	3.33	16.67	80
25	3.33	6.67	90

2005–06. The forecast (Fig. 6) indicated that SSTs in the Niño-3.4 region (Niño-3.4 is the box defined by 5°N–5°S, 120°–170°W) were likely to be above average during winter 2005–06. When the 3-month running mean of this temperature anomaly is above (below) 0.5°C for five consecutive months, the event is officially classified as an El Niño (La Niña). The version of this 3-month running mean in the Niño-3.4 region based upon version 2 of the Extended Reconstructed SST (ERSSTv.2; Smith and Reynolds 2005) dataset is called the oceanic Niño index (ONI; Kousky and Higgins 2007). CPC pays special attention to the status and future evolution of such events, because the impacts of both El Niño and its cold-SST counterpart, La Niña, have large and long-lasting impacts (up to a year) over the United States.

The forecaster must next place this information into the context of the other forecast tools and develop outlook maps. The four primary tools used in the DJF 2005–06 three-month temperature outlook (Figs. 7a–d) alternatively complement or contradict one another, and have widely varying magnitudes and a priori skill levels. Before the consolidation tool was implemented in early 2006, a forecaster was forced to combine all of this information subjectively, often in a less than optimal way, which was conducive to error and impossible to reproduce after the fact. Figure 7e shows the results of the objective consolidation of these four tools. As we will demonstrate later, armed with this starting point, the forecaster stands a much better chance of producing an outlook that better reflects the available information.

Seasonal total precipitation has at least several times more degrees of freedom, on average, than seasonal mean 2-m temperature (Richman and Lamb 1985; Livezey and Barnston 1988), and is a discontinuous field. These qualities make 3-month precipitation much more difficult to predict than temperature. Consequently, precipitation forecast tools (Figs. 8a–d) have much lower average skill and much lower area coverage than do those for temperature (Figs. 7a–d).

Uncertainty about the behavior of the tropical Pacific Ocean made the DJF 2005–06 outlook difficult. The text bulletin that accompanied the official forecasts for DJF 2005–06, made 17 November 2005 (not shown), indicates that, in spite of the observed existence of colder than normal sea surface and subsurface ocean temperatures in the eastern tropical Pacific, neutral ENSO conditions were considered to be likely to persist until early 2006.

5. Skill of LRF

A record of the skill of the forecast tools over a sufficiently long historical period is needed in order to properly weight the tools' contributions to operational forecasts. This, in turn, affects the magnitude of the forecast probabilities. CPC requires that any forecast tool must be accompanied by at least a 25-yr record of the forecast skill, in order to be used in the objective consolidation technique used in the forecast process. CPC also uses skill scores to document the temporal and spatial variability of skill, and to calibrate the subjective probabilities placed on the outlook maps. Finally, skill information can be used by those applying CPC outlooks to risk assessment (Livezey 1990).

The U.S. average Heidke skill score, which is the percent improvement of the forecast over climatology, or random forecasts, of ½-month-lead 3-month mean temperature outlooks from 1995 to 2005, is shown in Fig. 9. The dashed curve in the top graph (Fig. 9a), marked by "O" symbols, shows the U.S. average skill score for official outlooks (OFF), *not* including the EC regions on the map $s = [(c - e)/(t - e)]100$, where c is the number of grid points correct, e is the number of grid points expected correct by chance given the 30-yr climatology in effect when the forecast was issued, and t is the total number of grid points where non-EC prob-

TABLE 3. Tools and considerations in the ½-month- and zero-lead 1-month outlooks.

	1/2-month-lead 1-month outlook	Zero-lead 1-month outlook
Tools	OCN, CCA, SMLR, and CFS	OCN, CCA, SMLR, CFS, daily official forecasts for days 1–7, and CPC 6–10- and 8–14-day average outlooks
Factors considered	Climate signals, including ENSO, drought, SST near coasts, snow cover, and soil moisture	Climate signals, weather during the first 2 weeks of the forecast period

abilities were assigned. Henceforth, these scores will be referred to as NOEC scores. Thick curves in Fig. 9a, marked by an X, show the NOEC scores for the consolidation forecasts (CON). There is considerable variability in this score (Fig. 9a). The highest scores occur in association with ENSO events. The level dashed and thick lines indicate that the 1995–2005 average NOEC skill is in the low 20s for NOEC official forecasts and in the upper 20s for NOEC consolidation forecasts.

The skill for all grid points on the forecast map (combined non-EC and EC forecasts) is shown in bottom graph (Fig. 9b). The equation for this "all points," or "ALL" skill score (sometimes referred to as the modified Heidke skill score) is $s = \{[(c - e + (1/3)ec]/(t - e)\}100$, where c and e are as defined earlier, ec is the number of grid points predicted with "equal chances" (indicated by EC on the forecast maps in Fig. 1), and t is the total number of all of the grid points on the map. The ALL skill score (Fig. 9b) is more conservative than NOEC, weighting areas covered by probabilities greater than 33.3, as well as EC forecast regions. Successful forecasts with small non-EC probability regions and large EC regions necessarily have much lower (ALL) scores (Fig. 9b) in comparison with NOEC skill scores for the same forecasts (Fig. 9a).

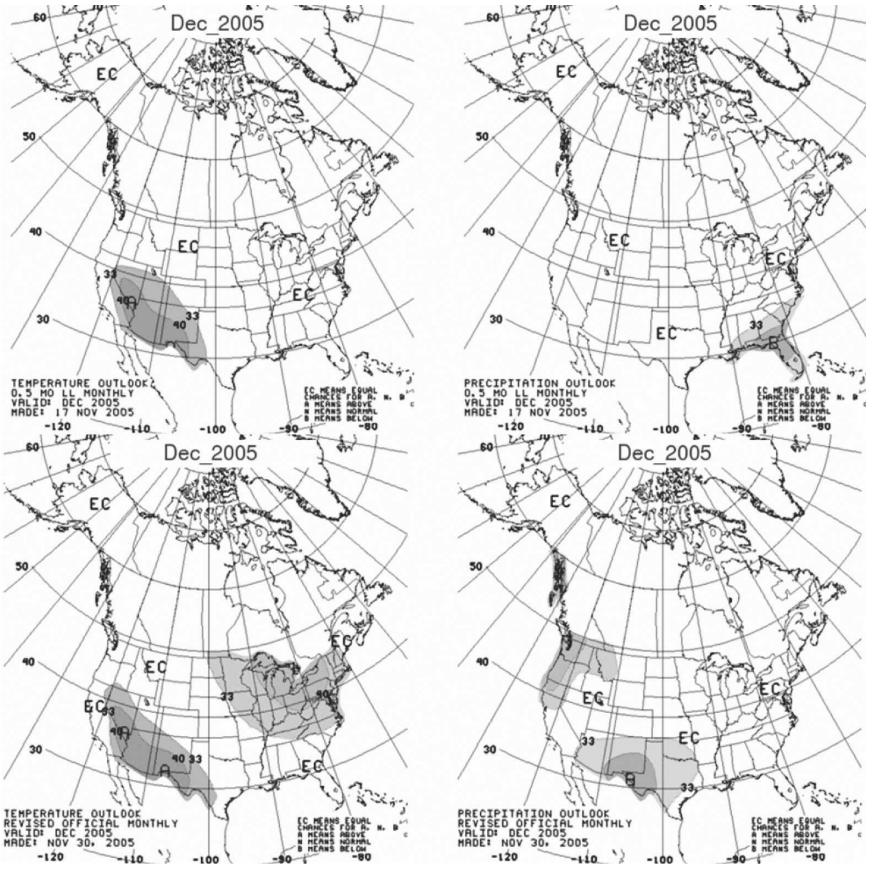


FIG. 4. (left) One-month temperature and (right) precipitation outlooks, at leads of (top) ½ month and (bottom) zero, valid for December 2005. The meaning of the contours and shading is the same as in Fig. 1.

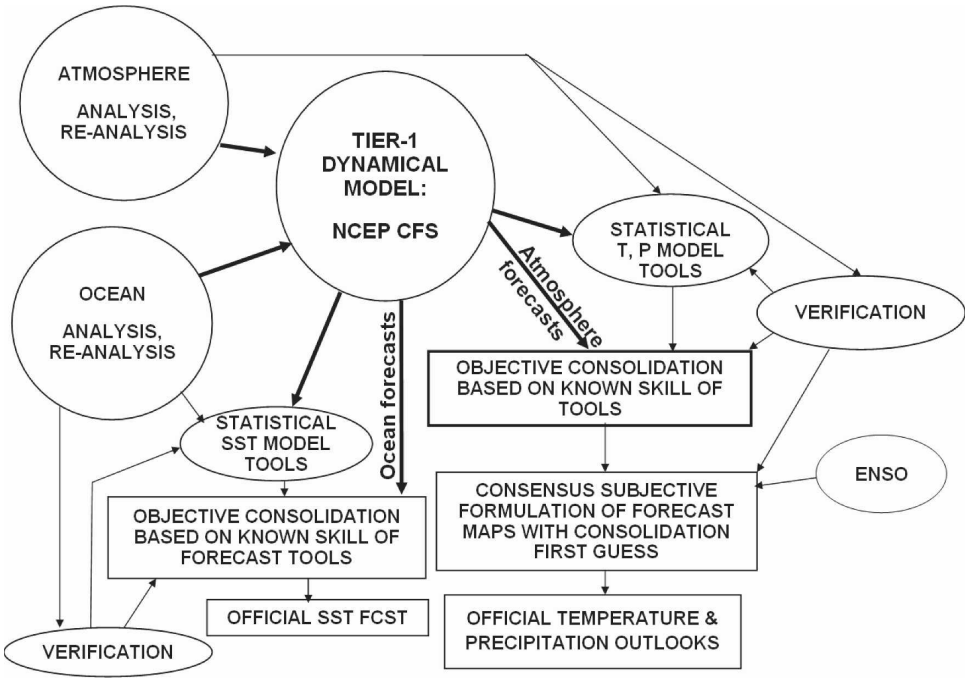


FIG. 5. NCEP 3-month outlook operation schematic.

During 1995–2005, the NOEC (ALL) skill scores indicate that CON temperature forecasts improve upon official forecasts by 18% (78%) (Figs. 9a and 9b). The improvement in the precipitation outlooks by CON over OFF is much larger, from a score of 4.1 (OFF) to 12.1 (CON) for NOEC forecasts, and from 1.0 (OFF) to 3.0 for ALL forecasts (Figs. 10a and 10b).

One reason for the improvement made by the CON

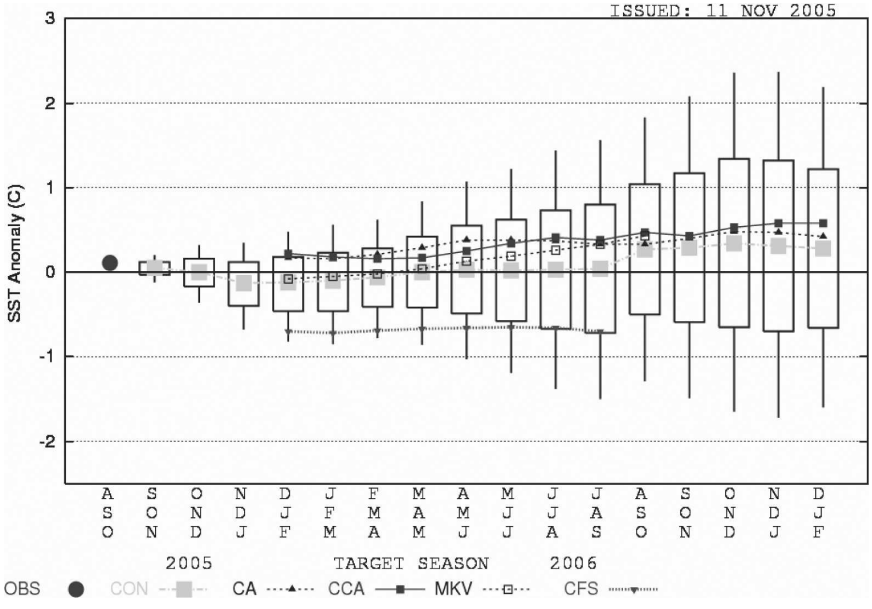


FIG. 6. Official SST outlook for the Niño-3.4 region, issued 11 Nov 2005. The box-and-whiskers plots show the official forecast, labeled CON, resulting from objectively combining constructed analog (CA), CCA, Markov (MKV), and CFS forecast tools. The large dot is the latest observed 3-month mean T. The top (bottom) of each box corresponds to the 84th (16th) percentile of the forecast distribution. Whiskers correspond to the 97.5th (2.5th) percentile of the expected forecast distribution.

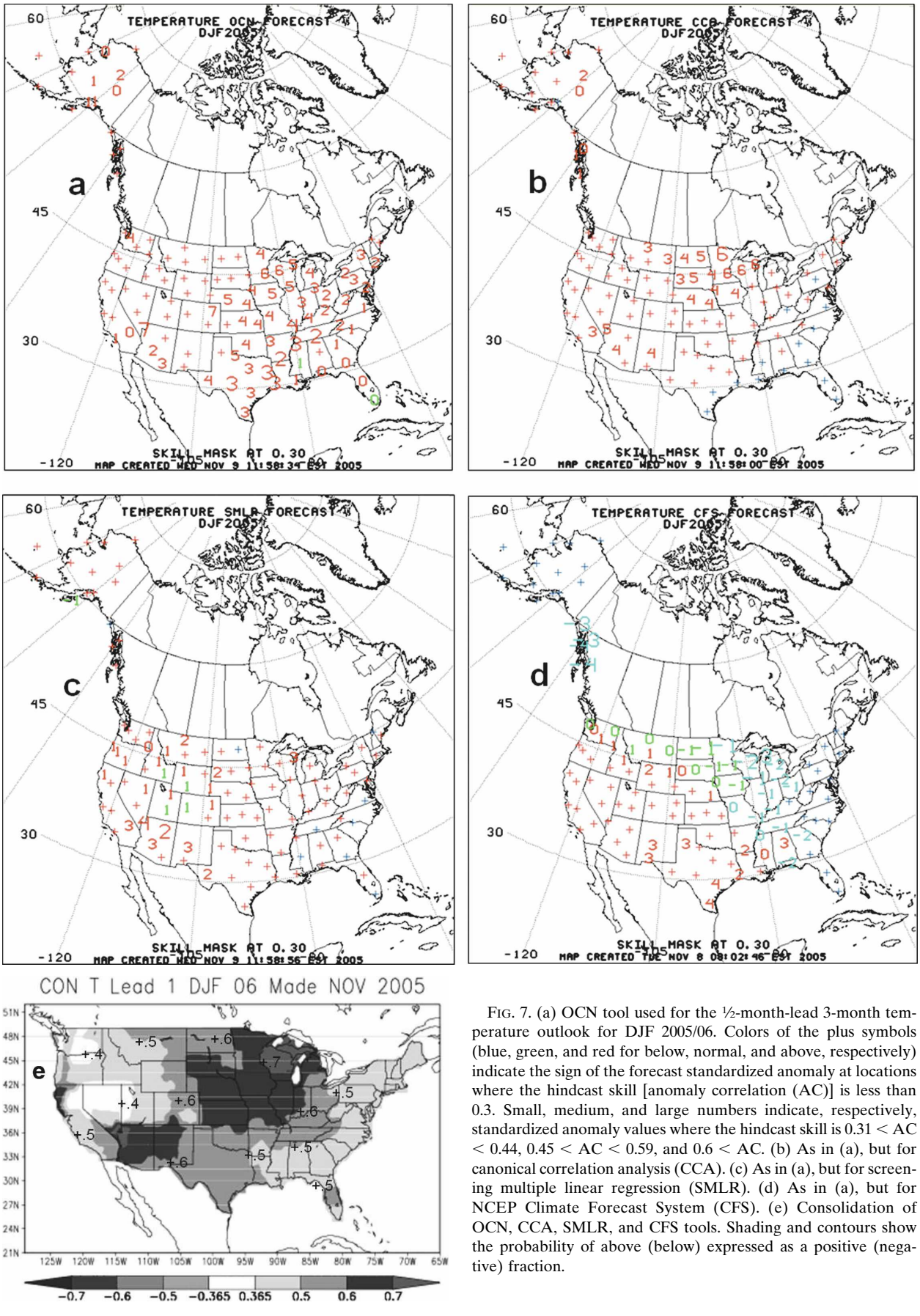


FIG. 7. (a) OCN tool used for the ½-month-lead 3-month temperature outlook for DJF 2005/06. Colors of the plus symbols (blue, green, and red for below, normal, and above, respectively) indicate the sign of the forecast standardized anomaly at locations where the hindcast skill [anomaly correlation (AC)] is less than 0.3. Small, medium, and large numbers indicate, respectively, standardized anomaly values where the hindcast skill is $0.31 < AC < 0.44$, $0.45 < AC < 0.59$, and $0.6 < AC$. (b) As in (a), but for canonical correlation analysis (CCA). (c) As in (a), but for screening multiple linear regression (SMLR). (d) As in (a), but for NCEP Climate Forecast System (CFS). (e) Consolidation of OCN, CCA, SMLR, and CFS tools. Shading and contours show the probability of above (below) expressed as a positive (negative) fraction.

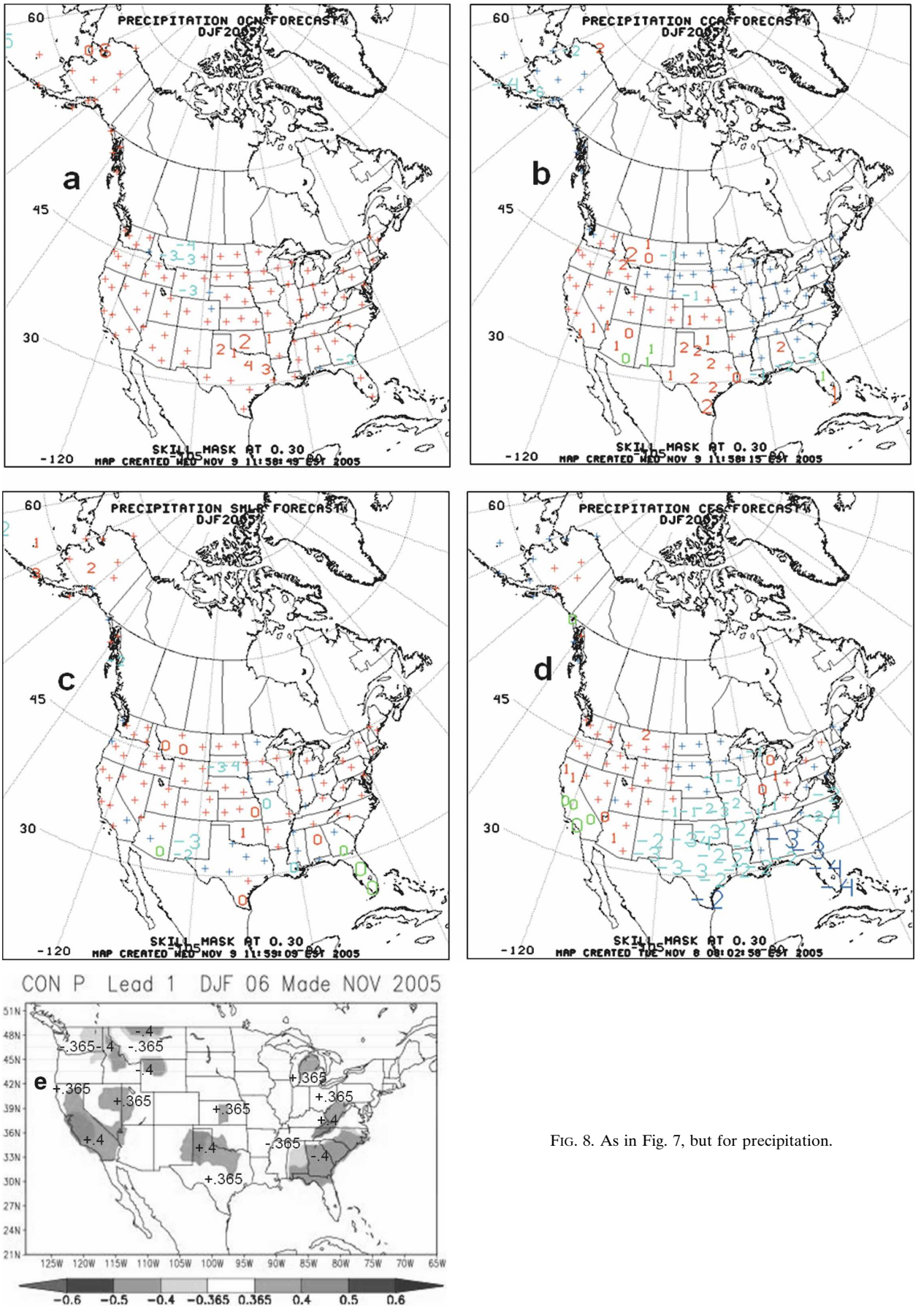


FIG. 8. As in Fig. 7, but for precipitation.

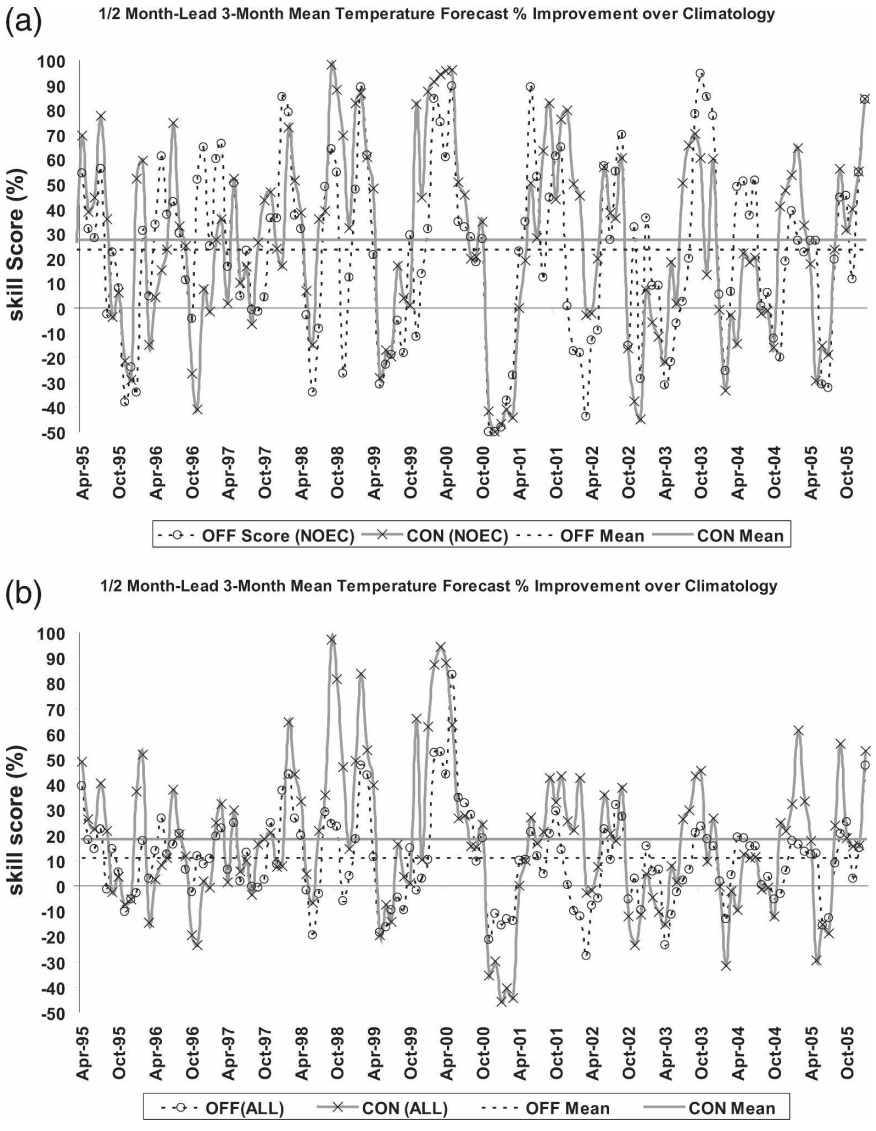


FIG. 9. (a) Percent improvement of the outlook over random (climatology) forecasts $s = [(c - e)/(t - e)]100$, where c = the number of points correct, e = the number of points expected correct by chance, t = the number of points in total for official real-time, operational, ½-month-lead, 3-month temperature outlooks (dashed curve), and retrospective outlooks made using CON (thick curve), for the period 1995–late 2005. Horizontal thick and dashed thin lines show the period averages for both forecast systems. Points used to compute this score come from regions that were *not* assigned to the equal chances (EC) category. (b) As in (a) but for all regions and using the form of the score $s = \{[c - e + (1/3)ec]/(t - e)\}100$, where ec = the number of points predicted to be EC.

over the official outlooks is that CON skillfully forecasts larger areas with greater than 33⅓% probability than is done in OFF. Another reason is that CON weights tools according to their skills in the immediate past. The skill used to do weighting in CON is estimated by an exponential moving average that approximates a running mean of about 30 yr. The weight assigned to each tool is objectively determined from this skill estimate (UVOC). The CON benefits from an objective and reproducible weighting procedure, while forecasters must estimate the weights on a case-by-case basis. For relatively low skill forecasts, any error in this subjective estimate is likely to degrade the resulting forecast. The CON accurately reflects the complementary,

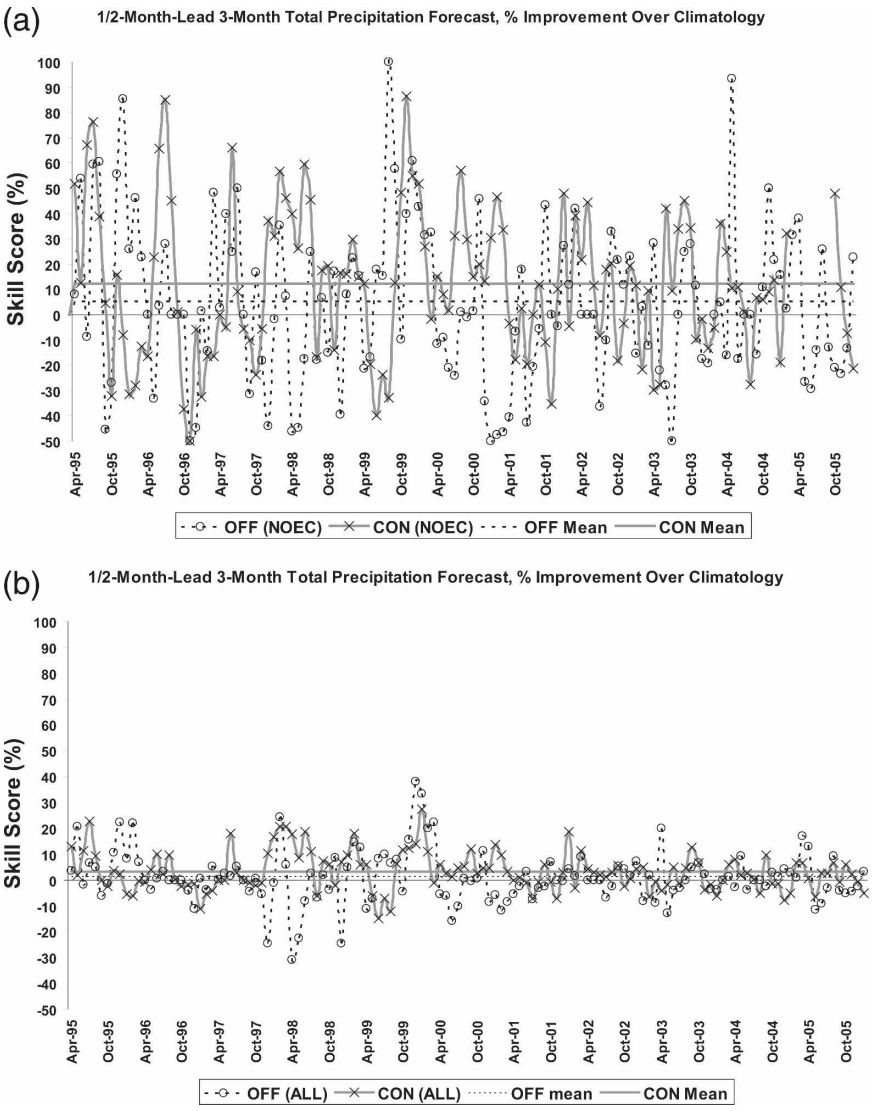


FIG. 10. As in Fig. 9, but for *P*.

redundant, or conflicting contributions to the forecast from multiple tools and consistently makes better use of the available forecast information over the 10 yr of real-time official and hindcast outlooks (1995–2005).

The consolidation provides a mechanism to constrain the subjectivity that formerly characterized CPC's seasonal outlook process. It also serves as a rational basis for accurately combining outlooks from a number of forecast tools. Since we have only been using the technique in operations for a year, it remains to be seen whether or not human forecasters can consistently improve upon this technique. But, the success we have seen so far is encouraging. We anticipate that the trend toward more objective methods of making outlooks at CPC will continue.

Another comparison of the NOEC skill of OFF and CON over 1995–2005 is shown in (Fig. 11). The graph shows considerable scatter about the regression line, but the slope indicates that there is a relationship between the skill of the two forecasts. The average (OFF, CON) point, indicated by the X on the graph, is at (22, 26), indicating that, on average over 1995–2005, CON improved upon OFF by about 18%. Because the slope of the regression line is less than 1, it intersects the dashed line bisecting the graph at the point where the skill of OFF equals the skill of CON (a score of about 32). To the left of that point along the regression line, the CON scores better than does OFF, while to the right of that point, the OFF scores better than CON. This property is implied in Fig. 9, by the fact that the

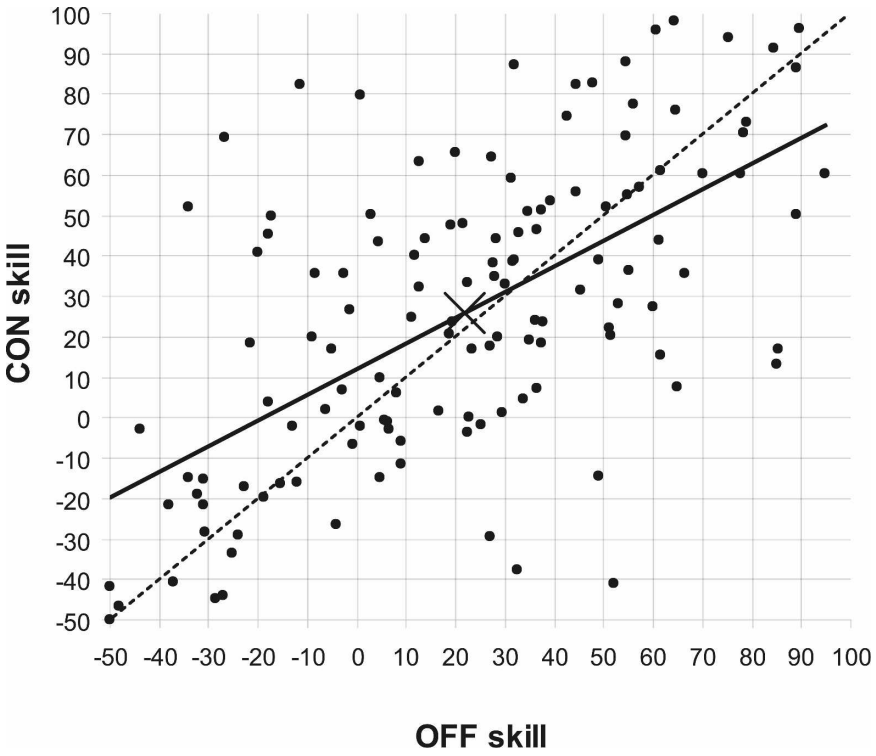


FIG. 11. Comparison of the conterminous U.S. average skill of official CPC ½-month-lead 3-month *T* outlooks for non-EC regions with that of outlooks made using an objective consolidation of four forecast tools over the 1995–2005 period. The skill score is the percent improvement of the outlooks over the expected scores of random forecasts. The solid line is the least squares regression fit. The dashed line divides the graph between outlooks for which CON is better than OFF, to the left, and OFF is better than CON, to the right. The average is indicated by an X.

OFF skill curve tends to be outside of CON for both the highest and lowest scoring forecasts. The fact that the slope of the regression line in Fig. 11 is less than 1 indicates that the official outlook has higher (lower) skill than the consolidation in high- (low-) scoring situations, such as ENSO (non-ENSO) events. This could be evidence, in part, of value added to official forecasts by forecasters during ENSO events when skill is generally high and, alternatively, of the real difficulty forecasters have in making subjective outlooks from tools characterized by subtle differences and very low expected skill.

The NOEC skill score (Figs. 9a, 10a, and 11) is non–area weighted. Thus, one can make forecasts at as few as one station and still get a very high score (the only scores possible in that case are +100 for a correct one-station forecast, 0 for an EC forecast, or −50 for an incorrect one-station forecast). The area-weighted, ALL skill score (Figs. 9b, 10b, and 11) is much more conservative, since it almost always incorporates grid points at which EC forecasts were made, damping the resulting score toward zero. Thus, a forecast with a high ALL skill score is potentially of much more value than one with a high NOEC score, since it represents the skill over the entire map, and it motivates using tools, such as the CON, which tend to forecast larger areas with greater-than-climatological probabilities.

The skill of the CON versus OFF ½-month-lead 3-month temperature outlooks using the ALL score (Fig. 12) indicates an even stronger relationship between the CON and OFF outlooks, less scatter, and a larger (78%) and more consistent improvement in the skill of CON in comparison with OFF. The average point for this graph is at (OFF, CON) = (10.2, 17.2), and is indicated by an X (Fig. 12). The improvement made by the CON over the OFF outlooks is amplified by the fact that CON forecasts cover 20% more area and have less area covered by equal chance than do the official outlooks (Fig. 13). This is good news for users of CPC outlooks, who have often noted that outlooks with less EC area on the map (along with more skill) are more useful. Finally, the area-weighted skill

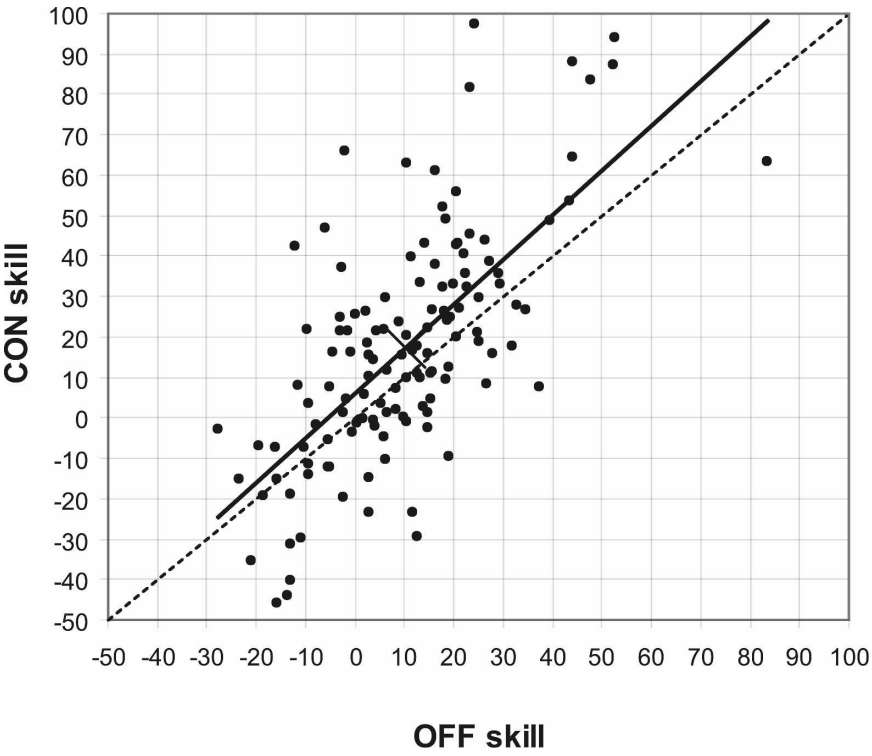


FIG. 12. Comparison of the conterminous U.S. average skill of official CPC ½-month-lead 3-month *T* outlooks for both EC and non-EC regions with that of objective outlooks made using a consolidation of four forecast tools over the 1995–2005 period. The skill score is the percent improvement of the outlooks over the expected scores of random forecasts. The solid line is the least squares regression fit. The dashed line divides the graph between outlooks for which CON is better than OFF, to the left, and OFF is better than CON, to the right. The average is indicated by an X.

score rewards forecasts that cover greater areas, while the non-EC version does just the opposite. These qualities make the area-weighted score a desirable alternative to the NOEC version, the 48-month running mean of which is the current official skill metric used by NOAA for the seasonal outlook. There is virtually no relationship between area covered and skill between CON and OFF outlooks during the 1995–2005 period (Fig. 13).

Scatter diagrams comparing the U.S. average skill of the OFF and CON ½-month lead forecasts of precipitation (not shown) have large scatter among the data points and indicate that the relationship between the CON and OFF forecasts is nearly nonexistent. However, because the skill of the precipitation outlooks is so much lower than that for temperature, the percentage improvement by the consolidation is that much greater. The (OFF, CON) average for NOEC forecasts is (4.1, 12.1). Thus, using CON over 1995–2005 produced an increase in skill for the official 3-month precipitation outlooks from an average of 4.1 to 12.1. For ½-month-lead 3-month precipitation outlooks, the corresponding ALL graph (not shown) has (OFF, CON) averages of (1.0, 3.0), a huge improvement, though the skill is quite low.

Figures 14 and 15 show the geographical distribution of the Heidke skill score of official non-EC, ½-month-lead 3-month temperature and precipitation outlooks for the 10 yr from 1995 to 2004. Average temperature skill is consistently high in the Southwest, reaching maximum values in excess of 70 in all seasons (Figs. 14a–d). That region also has a consistently high percentage of non-EC forecasts in all seasons, as indicated by the color shading. This result is not surprising, since the statistical forecast tools (OCN, CCA, and SMLR) have their highest skill there (Barnston 1994b), and there is a large trend signal there. The South and Southeast fare well in all but the fall (Fig. 14d) when the area covered by positive skill is lowest and the percentage of non-EC outlooks is also lowest. Average skill is negative in the Northeast and the Great Lakes in all seasons. Since few NOEC forecasts were made there, the score is based on just a few forecasts and is not a robust indicator of the actual possible skill. A map of the skill

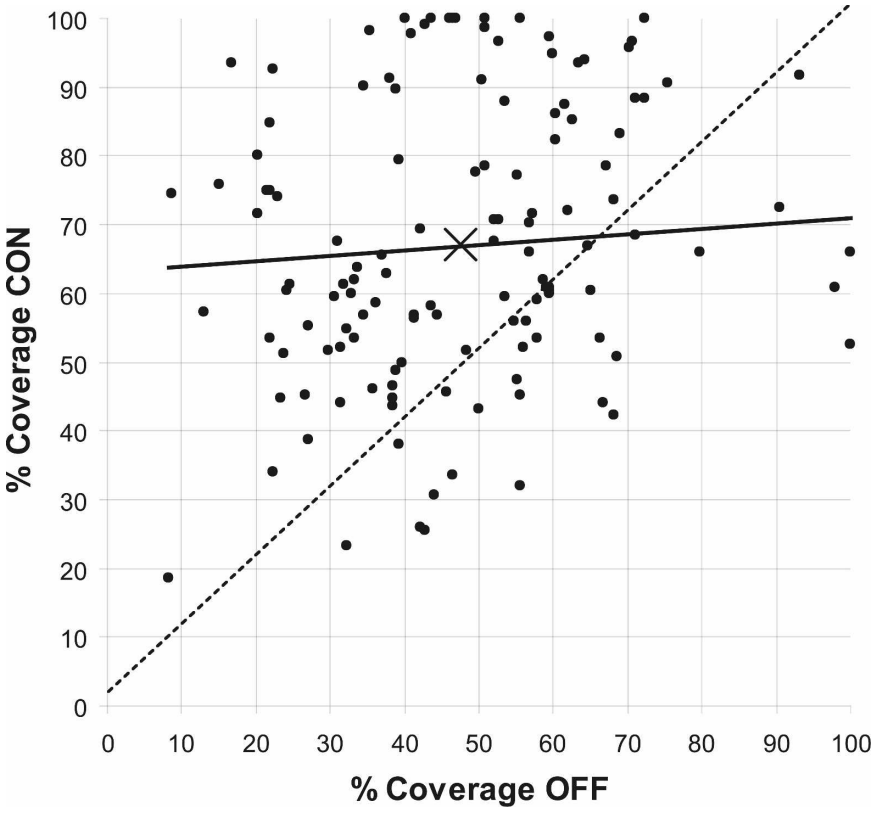


FIG. 13. Comparison of the conterminous U.S. percent coverage of official CPC ½-month-lead 3-month temperature outlooks for non-EC regions with that of outlooks made using an objective consolidation of four forecast tools over the 1995–2005 period. The solid line is the least squares regression fit. The dashed line divides the graph between outlooks for which CON covered more map area than OFF, to the left, and for which OFF covered more map area than CON, to the right. The average is indicated by an X.

of CON forecasts (not shown) indicates that this low-skill region is where the technique produces the largest improvement. We are, therefore, optimistic that the skill scores of official forecasts in these regions will improve through the use of the consolidation.

One-half-month-lead 3-month precipitation outlooks have much lower U.S. average skill scores and a much smaller percentage of non-EC forecasts (Fig. 15) in comparison with the corresponding temperature outlooks (Fig. 14). However, relatively high wintertime precipitation skill, and percentage of forecasts (Fig. 15a), are found in the West, especially the Northwest and Southwest, and also the southern United States. These regions of high skill are consistent with ENSO precipitation patterns. This skill distribution is also evident in the spring scores (Fig. 15b), though only over the South. During summer and fall the skill is best in the West and the South (Figs. 15c and 15d). Skill is positive in the Northeast in both spring and fall, while in the Great Lakes, it is highest in the summer.

6. Conclusions

Outlooks of 1- and 3-month average temperature and total precipitation have been made operationally since 1946 and 1982, respectively. The scientific basis for these products has changed from one based entirely on 1) skill derived from predictability during the first week of a zero-lead forecast, 2) persistence, and 3) low-frequency signals implied by often-weak lagged correlations between antecedent conditions and subsequent seasonal anomalies, to one based mainly on 1) ENSO; 2) trend; 3) dynamics of low-frequency ocean–atmosphere variability, as simulated by dynamical models and facilitated by new observing systems, including satellites and the Tropical Ocean Global Atmosphere Tropical Atmosphere–Ocean (TOGA-TAO) array; and 4) low-frequency signals derived from linear statistical techniques.

Production methods have also changed. Early outlooks (1946–81) were composed through entirely subjective methods, similar to those used by short-range

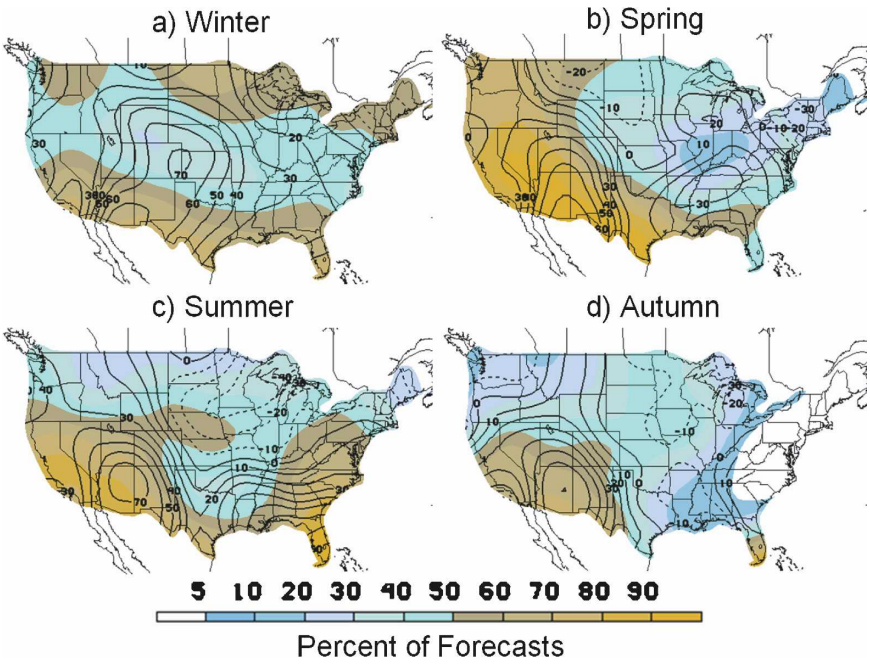


FIG. 14. Non-EC Heidke skill score (contours: solid, positive; dashed, negative) of ½-month-lead 3-month official temperature outlooks for (a) winter (DJF), (b) spring (MAM), (c) summer (JJA), and (d) autumn (SON) for outlooks valid during JFM 1995–DJF 2004. Shading gives the percent of all outlooks that were non-EC. Regions with less than 5% of outlooks are white.

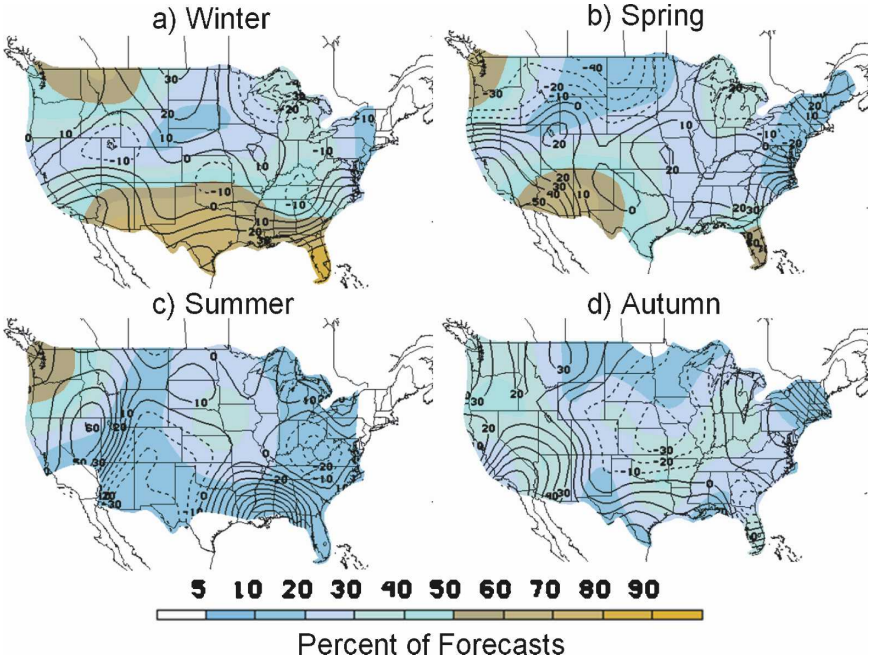


FIG. 15. Non-EC Heidke skill score (contours: solid, positive; dashed, negative) of ½-month-lead 3-month official precipitation outlooks for (a) winter (DJF), (b) spring (MAM), (c) summer (JJA), and (d) autumn (SON) for outlooks valid during JFM 1995–DJF 2004. Shading gives the percent of all outlooks that were non-EC. Regions with less than 5% of outlooks are white.

forecasters of the day. Modern methods include the use of long histories of outlooks and verifications from prior years (reforecasting) to allow bias removal, and display of forecast information only where and when an acceptable level of skill has been found in the historical record (skill masks), and the further use of the skill record to weight the contribution of forecast tools to a consolidation of those tools. The consolidation technique was formally introduced into CPC forecast operations in early 2006. Consolidation of forecast tools raises the skill of retrospective (1995–2005) seasonal, ½-month-lead temperature outlooks from an average improvement over climatology of 22% (official) to 26% (consolidation) and raises precipitation outlooks from an average improvement upon climatology of 4% (official) to 12% (consolidation, non-EC Heidke skill score).

The format of the outlooks has changed, from strictly categorical outlook maps in the early days to one of probabilistic maps, augmented by maps and graphs, based upon the probability of exceedance, which give highly detailed information about the implications of the outlook for the full probability distribution.

Finally, CPC's 1- and 3-month outlook probability maps are being placed onto the National Digital Forecast Database (NDFD). This will allow users to download gridded (in General Regularly-distributed Information in Binary format, second edition; GRIB2) datasets with 5 km × 5 km resolution in a variety of formats, including Extensible Markup Language (XML), Hypertext Markup Language (HTML), and Geographic Markup Language (GML). This capability will give users unprecedented access to the outlooks and immensely increase users' ability to create their own graphical renderings of the outlooks.

With these important pieces in place, NWS operational LRFs are making increasingly better use of observed and forecast information, combined through more objective methods, and are increasingly accessible, in more forms, to users. Future increases in skill are more likely to come from, and be more clearly related to, improvements in the forecast tools and to our increasing understanding of the physics of low-frequency variability as incorporated into the tools. These developments make CPC's LRFs more science based, objective, independently reproducible, and accessible. All of these qualities increase the real value of these outlooks to current and potential users of the product, whom we are increasingly engaging in a dialogue that informs both sides about how the outlooks can and cannot be used, what our mutual needs are, and how we can meet those needs as a community.

APPENDIX

Anomaly Correlation

The anomaly correlation (AC) is a measure of similarity between forecast and observed maps:

$$\mathrm{AC} = \frac{\sum_{i=1}^{n} (f_i)(a_i)/n}{\sqrt{\sum_{i=1}^{n} (f_i)^2/n \sum_{i=1}^{n} (a_i)^2/n}},$$

where F_i is the forecast, A_i is the analysis (observation), C_i is the climate, $f_i = F_i - C_i$, $a_i = A_i - C_i$, and n is the number of points.

REFERENCES

Barnston, A. G., 1994a: Linear statistical short-term climate predictive skill in the Northern Hemisphere. *J. Climate,* **7,** 1513–1564.

——, 1994b: New long-lead forecasts: Seasonal and geographic variations in skill. *Proc. 19th Climate Diagnostics Workshop,* College Park, MD, NOAA/NWS, 412–415. [NTIS PB95-225546.]

——, and R. E. Livezey, 1987: Classification, seasonality and persistence of low frequency atmospheric circulation patterns. *Mon. Wea. Rev.,* **115,** 1083–1126.

——, and Coauthors, 1994: Long-lead seasonal forecasts—Where do we stand? *Bull. Amer. Meteor. Soc.,* **75,** 2097–2114.

——, A. Leetmaa, V. E. Kousky, R. E. Livezey, E. A. O'Lenic, H. M. Van den Dool, A. J. Wagner, and D. A. Unger, 1999: NCEP forecasts of the El Niño of 1997–98 and its U.S. impacts. *Bull. Amer. Meteor. Soc.,* **80,** 1829–1852.

Blackmon, M. L., 1976: A climatological spectral study of the 500 mb geopotential height of the Northern Hemisphere. *J. Atmos. Sci.,* **33,** 1607–1623.

——, J. M. Wallace, N.-C. Lau, and S. J. Mullen, 1977: An observational study of the Northern Hemisphere wintertime circulation. *J. Atmos. Sci.,* **34,** 1040–1053.

——, Y. H. Lee, and J. M. Wallace, 1984a: Horizontal structure of 500 mb height fluctuations with long, intermediate and short time scales. *J. Atmos. Sci.,* **41,** 961–979.

——, ——, ——, and H. H. Hsu, 1984b: Time variation of 500 mb height fluctuations with long, intermediate and short time scales as deduced from lag-correlation statistics. *J. Atmos. Sci.,* **41,** 981–991.

Gilman, D. L., 1985: Long-range forecasting: The present and the future. *Bull. Amer. Meteor. Soc.,* **66,** 159–164.

Guttman, N. B., and R. G. Quayle, 1996: A historical perspective of U.S. climate divisions. *Bull. Amer. Meteor. Soc.,* **77,** 293–303.

Higgins, R. W., A. Leetmaa, Y. Xue, and A. Barnston, 2000a: Dominant factors influencing the seasonal predictability of U.S. precipitation and surface air temperature. *J. Climate,* **13,** 3994–4017.

——, J.-K. E. Schemm, W. Shi, and A. Leetmaa, 2000b: Extreme precipitation events in the western United States related to tropical forcing. *J. Climate,* **13,** 793–820.

——, A. Leetmaa, and V. E. Kousky, 2002: Relationships between climate variability and winter temperature extremes in the United States. *J. Climate,* **15,** 1555–1572.

Horel, J. D., and J. M. Wallace, 1981: Planetary-scale atmospheric

phenomena associated with the Southern Oscillation. *Mon. Wea. Rev.,* **109,** 813–829.

Huang, J., and H. M. Van den Dool, 1996: Analysis of model-calculated soil moisture over the United States. *J. Climate,* **9,** 1350–1362.

——, ——, and A. G. Barnston, 1996: Long-lead seasonal temperature prediction using optimal climate normals. *J. Climate,* **9,** 809–817.

Ji, M., A. Kumar, and A. Leetmaa, 1994: A multiseason climate forecast system at the National Meteorological Center. *Bull. Amer. Meteor. Soc.,* **75,** 569–577.

Kalman, R. E., 1960: A new approach to linear filtering and prediction problems. *Trans. ASME J. Basic Eng.,* **82,** 35–45.

Kousky, V. E., and R. W. Higgins, 2007: An alert classifications system for monitoring and assessment of the ENSO cycle. *Wea. Forecasting,* **22,** 353–371.

Livezey, R. E., 1990: Variability of skill of long-range forecasts and implications for their use and value. *Bull. Amer. Meteor. Soc.,* **71,** 300–309.

——, and A. G. Barnston, 1988: An operational multi-field analog/anti-analog prediction system for United States seasonal mean temperatures. Part 1: System design and winter experiments. *J. Geophys. Res.,* **93,** 10 953–10 974.

——, and T. M. Smith, 1999: Covariability of aspects of North American climate with global sea surface temperatures on interannual to interdecadal timescales. *J. Climate,* **12,** 289–302.

——, J. D. Hoopingarner, and J. Huang, 1995: Verification of official monthly mean 700-hPa height forecasts: An update. *Wea. Forecasting,* **10,** 512–527.

Lorenz, E. N., 1982: Atmospheric predictability experiments with a large numerical model. *Tellus,* **34,** 505–513.

Mo, K. C., and R. E. Livezey, 1986: Tropical–extratropical geopotential height teleconnections during the Northern Hemisphere winter. *Mon. Wea. Rev.,* **114,** 2488–2515.

Namias, J., 1953: *Thirty-Day Forecasting: A Review of a Ten-Year Experiment. Meteor. Monogr.,* No. 6, Amer. Meteor. Soc., 83 pp.

National Research Council, 2001: *A Climate Services Vision: First Steps toward the Future.* National Academy Press, 84 pp.

——, 2003: *Fair Weather: Effective Partnerships in Weather and Climate Services.* National Academy Press, 220 pp.

O'Lenic, E. A., 1994: A new paradigm for production and dissemination of NWS' long-lead-time seasonal climate outlooks. *Proc. 19th Climate Diagnostics Workshop,* College Park, MD, NOAA/NWS, 408–411. [NTIS PB95-225546.]

Rasmusson, E. M., and T. H. Carpenter, 1982: Variations in tropical sea surface temperature and surface wind fields associated with the Southern Oscillation/El Niño. *Mon. Wea. Rev.,* **110,** 354–384.

Richman, M. B., and P. J. Lamb, 1985: Climatic pattern analysis of three- and seven-day summer rainfall in the central United States: Some methodological considerations and a regionalization. *J. Climate Appl. Meteor.,* **24,** 1325–1343.

Saha, S., and Coauthors, 2006: The NCEP Climate Forecast System. *J. Climate,* **19,** 3483–3517.

Simmons, A. J., J. M. Wallace, and G. W. Branstator, 1983: Barotropic wave propagation and instability, and atmospheric teleconnection patterns. *J. Atmos. Sci.,* **40,** 1363–1392.

Smith, T. M., and R. W. Reynolds, 2005: A global merged land–air–sea surface temperature reconstruction based on historical observations (1880–1997). *J. Climate,* **18,** 3450–3469.

Unger, D. A., 1997: Regional sources of predictive information for long-lead seasonal forecasts. *Proc. 22nd Annual Climate Diagnostics and Predictions Workshop,* Berkley, CA, NOAA/NWS, 367–370. [NTIS PB97159164.]

Van den Dool, H. M., 1994: New operational long-lead seasonal climate outlooks out to one year: Rationale. *Proc. 19th Climate Diagnostics Workshop,* College Park, MD, NOAA/NWS, 405–407. [NTIS PB95-225546.]

——, 2007: *Empirical Methods in Short-Term Climate Prediction.* Oxford University Press, 215 pp.

——, H. J. Huang, and Y. Fan, 2003: Performance and analysis of the constructed analogue method applied to U.S. soil moisture over 1981–2001. *J. Geophys. Res.,* **108,** 8617, doi:10.1029/2002JD003114.

Wallace, J. M., and D. L. Gutzler, 1981: Teleconnections in the geopotential height field during the Northern Hemisphere winter. *Mon. Wea. Rev.,* **109,** 784–812.

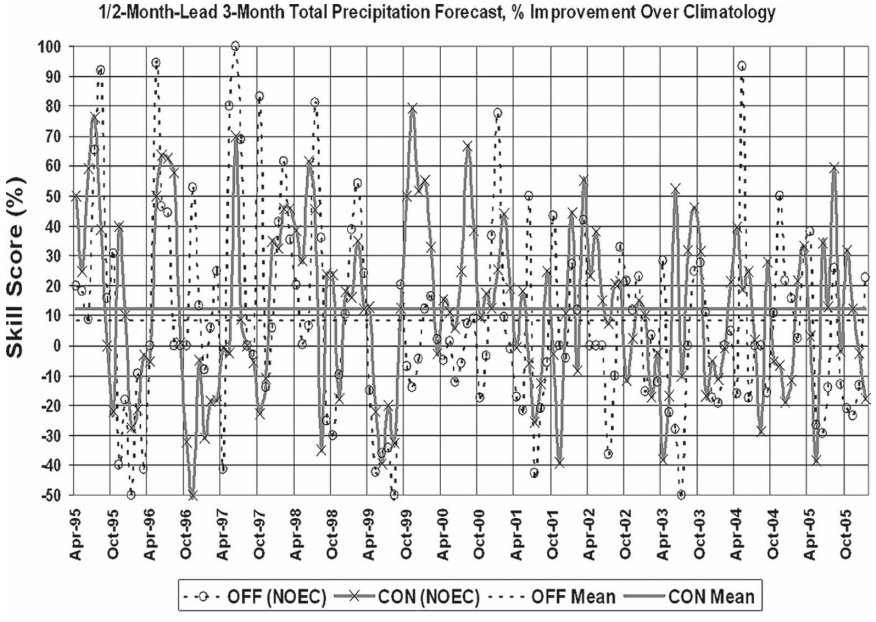
Wilks, D. S., 1995: *Statistical Methods in the Atmospheric Sciences.* Academic Press, 467 pp.

CORRIGENDUM

EDWARD A. O'LENIC, DAVID A. UNGER, MICHAEL S. HALPERT, AND KENNETH S. PELMAN

National Oceanic and Atmospheric Administration/National Weather Service/Climate Prediction Center, Camp Springs, Maryland

In O'Lenic et al. (2008) we underestimated the skill of both the official (OFF) and the consolidation (CON) precipitation forecasts for 1995–2005. The actual average skill of the OFF and CON forecasts over the period was 8.8 and 12.0, respectively. This means that the improvement by the CON was 36%, instead of 195%. Figure 10a was also in error. A corrected Fig. 10a is shown.



REFERENCE

O'Lenic, E. A., D. A. Unger, M. S. Halpert, and K. S. Pelman, 2008: Developments in operational long-range climate prediction at CPC. *Wea. Forecasting,* **23,** 496–515.

© 2008 American Meteorological Society